Deformation characteristics of the main embankments of the Qinghai-Tibet Railway in permafrost regions

FujunNiu[1], Minghao Liu[1, 2], Libo Wu[1, 2], GuodongCheng[1], QingbaiWu[1]
1 State Key Laboratory of Frozen Soil Engineering, Cold and Arid Regions Environmental and Engineering Research Institute, Chinese Academy of Sciences, Lanzhou, China
2 University of Chinese Academy of Sciences, Beijing, China

ABSTRACT
A principle of 'cooling roadbed' was applied during the construction of the Qinghai-Tibet Railway (QTR) in permafrost regions. The main embankments include crushed-rock basement embankment (CRBE), crushed-rock sloped embankment (CRSE) and U-shaped crushed-rock embankment (UCRE), along with traditional embankment (TE). Eleven years of monitored data show that, the deformation of all the embankments generally show as settlement. Among the four types of the embankments, the CRBE has a maximum settlement with a value of more than 31 cm. The deformations are related to geological conditions of the underlain permafrost, thermal regimes of the roadbeds. For an embankment, different deformations occur in the two shoulders with north-facing slope and south-facing slope. Therefore, considering the mechanical stability, cooling effect, symmetry of the ground temperature regime, material property and construction technique, UCRE can be recommended for future application. And also some improvement measures for the other embankment structures are proposed.
RÉSUMÉ
Une méthode de mitigation à la dégradation du pergélisol sous des infrastructures appelée 'fondation refroidissante' a été utilisée lors de la construction du chemin de fer du Qinghai-Tibet en zone de pergélisol de haute altitude en Chine. Différents types de fondation ont été testés: la fondation en enrochement concassé (FEC), les accotements en enrochement concassé (AEC), l'enrochement concassé en forme de U dans la fondation (ECUF) et la fondation standard (FS). Après 11 années de suivi de la performance de ces fondations, tous les remblais sont affectés par des tassements. Les tassements les plus importants supérieurs à 31 cm ont été observés dans la FEC. Ces tassements sont dus aux conditions du pergélisol sous le remblai et ils sont contrôlés par le régime thermique du remblai. En outre, les tassements observés sont différents pour les accotements orientés au nord et au sud des remblais. En tenant compte de la stabilité mécanique, de l'effet de refroidissement, de la symétrie du régime thermique du sous-sol, des propriétés des matériaux et des techniques de construction, l'ECUF est recommandé pour les prochaines applications. Des améliorations sont aussi proposées à cette méthode de mitigation.

1 INTRODUCTION

The Qinghai-Tibet Railway (QTR), as the world's highest and longest plateau railroad, is 1,142 km in length, crossing approximately 550 km of continuous permafrost regions. About 50% of the permafrost area traversed by the QTR is warm permafrost with a mean annual ground temperature (MAGT) of−1 to 0°C, and around 40% is ice-rich permafrost (Cheng, 2005). Under climate warming and regional permafrost degradation on the Qinghai-Tibet Plateau (QTP) (Wu et al., 2004), the changing thermal regime of the underlying permafrost would continuously influence the roadbed stability and its long-term operation (Wu et al., 2004). To overcome the engineering problems caused by permafrost changes and ensure the roadbed stability, an active-cooling principle had been proposed for construction of the QTR (Cheng, 2003), and various cooling measures, including crushed rock embankment (CRE), duct-ventilated embankment, sun-shading embankment and thermo-syphon embankment, have been tested and applied in the QTR (Ma et al., 2002; Cheng, 2008).

Although many studies have discussed the thermal regimes of embankments with different configurations (Niu et al., 2004, 2006; Feng et al., 2006; Cheng et al., 2008; Mu et al., 2012; Ma et al., 2009), there is nearly no report on deformation of the roadbed up to now. In fact, the deformation can much more directly reflect mechanical stability and the serving status.

The QTR was opened to serve with a train-speed of 100 km/h, one of the designed requirements. In this paper, we chose 4 typical embankments built in Chuma'erhe region along the QTR to analyze their deformation characteristics, based on 10 years' data monitored since 2003, just when the embankments were constructed. Based on the monitoring data, the deformation characteristics of the embankments, including 3 types of the CRE and one traditional embankment (TE), were analyzed and compared. The purpose is to evaluate the long-term stability of different embankment structures of the QTR, and assess the effects of the cooling principle for stabilizing the permafrost roadbed.

In order to monitor permafrost conditions under the embankments, 12 monitoring sections were installed along the QTR (K1,035+324 to K1,058+770), just after the roadbeds were constructed in 2003. All the 12 monitoring sections were located in the Chuma'er High Plain, the hinterland of the QTP (Figure 1). This region is characterized by a flat topography and widely distributed thermokarst lakes. The average elevation of the site is over 4,500 m. According to a meteorological station in this site, the mean annual air temperature (MAAT) is around

−4.5°C, and the frozen period is from September to April. The mean annual precipitation is about 300 mm, while the potential evaporation is 1,500−1,800 mm. There is sparse vegetation in this region, with less than 35% surface vegetation coverage. According to the geologic drilling data, permafrost under the monitored embankments are usually warm and ice-rich, with a MAGT of −1.28 to −0.70°C; the permafrost table ranges from 2.0 to 2.8 m in buried depth, and the volumetric ice content is about 40% at the depth from 2.8 to 6.0 m. The ground surface is covered by sand with gravels with a thickness of 1.0−2.0 m, and then underlain by silty clay with a thickness of 2.0−4.0 m. Fine sand is at the depth of 5.0 to 7.0 m, and sandstone or muddy sandstone is from 7.0 to 15.0 m. Three structures of crushed rock embankments: (1) crushed-rock basement embankment (CRBE), (2) crushed-rock sloped embankment (CRSE) and (3) U-shaped crushed-rock embankment (UCRE) (Figure 2(a), (b) and (c), respectively), and one traditional embankments (TE) (Figure 2(d)) that were constructed with normal gravel fill are selected for this study. All four embankment orientations are approximately northeast to southwest; therefore, the amount of solar radiation absorbed by the slope surface will differ between the sunny (left) and shady (right) embankment slopes.

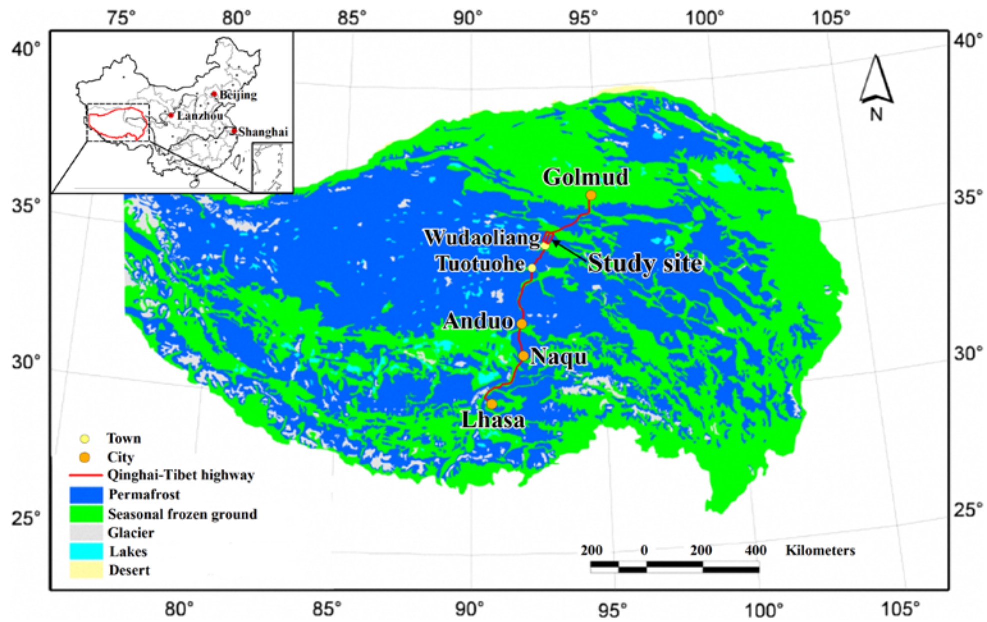

Figure 1. Location of the study site in the continuous permafrost zone of the QTP

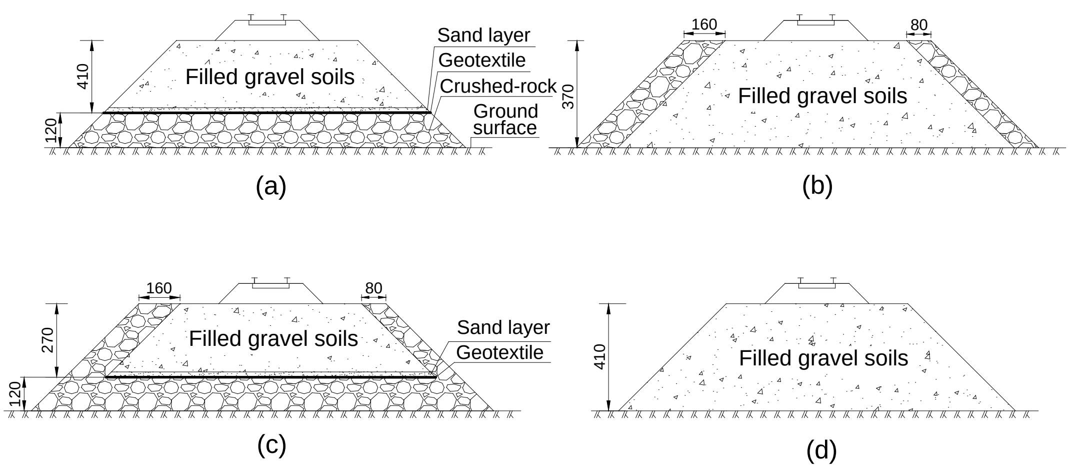

Figure 2. Structural diagrams of the monitored crushed rock embankments and traditional embankment (unit: cm). (a) CRBE; (b) CRSE; (c) UCRE; (d) TE

2 METHODOLOGY

Embankment deformation monitoring was done manually on a monthly basis. At every monitoring profile, illustrated in Figure 3a, 8 monitoring points and one reference point were installed on the embankment surface. The 8 monitoring points were made by 30 cm long nails and embedded into embankment shoulder totally. These points were arranged as four rows with rows pacing of 20 m, and then in every row there were 4 points respectively representing left shoulder and right shoulder. The reference point was also located on the embankment shoulders. At the point, a longer metal rod was embedded into the embankment by 20m deep with upper end exposed on the embankment surface. By subtracting the elevation of the monitoring point from that of the reference point, a time series of embankment deformation can be gained from elevation differences.

Between July and September 2003, four 16-m depth boreholes were drilled at the two shoulders and the two slope toes of each monitored railway embankments. Another borehole, 16-m deep, was drilled in undisturbed natural ground 6–10 m away from the embankment toe (Figure 3b). Only the TE had two boreholes drilled in natural ground, on either side of the embankment and both were 10 m away from the embankment toe. A thermistor cable, with 33 thermistors at 0.5 m intervals from the surface down to 16 m, was installed within each borehole. The thermistors, with a precision of ±0.02°C, were manufactured and assembled by the State Key Laboratory of Frozen Soil Engineering. The ground temperature data was collected manually by a CR3000 data logger two times a month. Monitoring started in October 2003, just after the roadbeds were constructed. Data in 2008 were missing as the monitoring work was suspended for one year.

In addition, the left and right shoulders of embankment are determined from Golmud to Lhasa direction, meaning that right side slope and left slope of the embankment is always north-facing slope and south-facing slope.

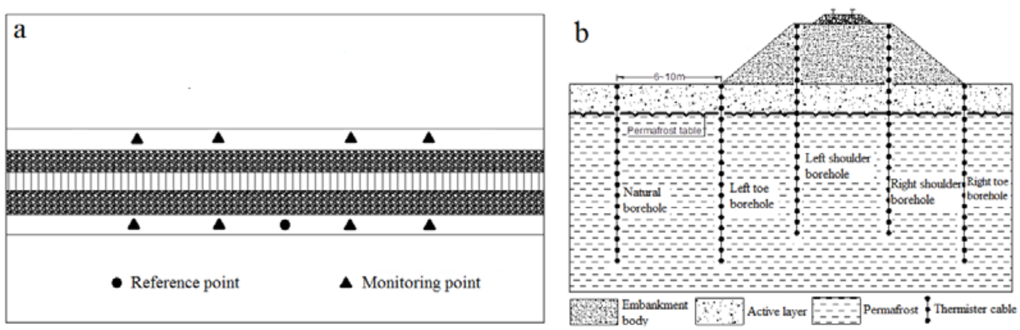

Figure 3. Location of the temperature observation boreholes and embankment deformation points in a typical monitoring section. (a) Distribution of monitoring points and reference point (vertical view); (b) Distribution of ground temperature boreholes in cross section.

3 RESULTS

3.1 Traditional Embankments (TE)

Monitoring profiles DK1053+315 was taken as an example to analyze the process of embankment settlements on TE. The settlement of embankment shoulders from 2003-2014 at monitoring section DK1053+315 was illustrated in Figure 4a. Figure 4a shows that both left and right shoulder had experienced significant settlement at the past 11 years. And meanwhile, differential settlements occurred between right and left shoulders of this embankment. From July 2003 to April 2014, the settlements on right and left embankment shoulders were 55 and 95 mm, respectively, meaning that mean annual settlement rate (MASR) of the embankment were about 4.5 and 8.6 mm/a. In addition, the main settlement occurred within the first 4 years after the monitoring system was installed. From 2003 to 2007, the settlement on right shoulder was 41 mm and on left shoulder was 55 mm, which account for about 58-75% of the total settlements.

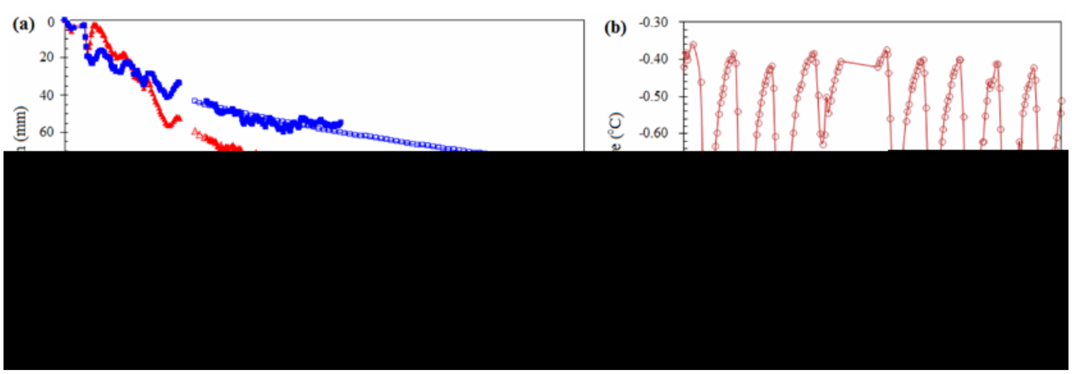

[redacted]

Figure 4. Deformation and ground temperature at section K1053+315. (a) the field measured and predicted embankment settlement; (b) ground temperature changes at depths of 5 and 10 m on right shoulder.

In order to analyze the long-term variations of embankment settlements, we used a trend line to predict the embankment settlements at section DK1053+315 (Figure 4a). The following trend line function was obtained from curve fitting with the monitoring data from 2006 to 2014:

$$Ln (S) = a \ln (Y) + b \quad [1]$$

where S is the total embankment settlements (mm), Y is the monitoring period (years), a and b are fitting parameters. The degree of fittings for right and left embankment shoulders were 0.84 and 0.96, which indicate the good fitting results. According to the predicted results in Figure 4a, the total embankment settlements on right and left embankment shoulders would possibly reach 78 and 145 mm, respectively, meaning that the increased settlements on left embankment shoulder are obviously large than that on right embankment shoulder.

Ground temperature monitoring at depths of 5 and 10 m in right shoulder of section DK1053+315 was shown in Figure 4b. Depths were measured from the original ground surface, with 5 m and 10 m representing shallow and deep permafrost respectively. The missing data from 2008 to 2009 do not impact the trends. Figure 4b indicates that deep permafrost under the right shoulders experienced obvious warming trends, while the temperature of shallow permafrost not changed too much. Permafrost temperature at depth of 10 m had increased 0.19 °C from 2003 to 2013.

3.2 Crushed-rock Basement Embankment (CRBE)

The process of embankment settlements of a typical CRBE at section DK1041+258 was shown in Figure 5a. Both embankment shoulders had experienced significant settlement from 2003 to 2014, especially the left shoulder. The settlement on left embankment shoulder in the past 11 years was 380 mm, which is nearly quadruple of the value on the right shoulder. In addition, the settlement on the left shoulder showed as sustained increase while the settlement on the right shoulder mainly occurred before 2007. From 2003 to 2006, the settlement on right shoulder was about 90 mm, account for over 90 % of the total settlements. As the method illustrated above, the predicted embankment settlements in both two shoulders were also showed in Figure 5a. The figure indicates that the embankment settlements on right shoulder will become stable, while the settlements in left embankment may increase significantly and reach to 600 mm by the year 2023.

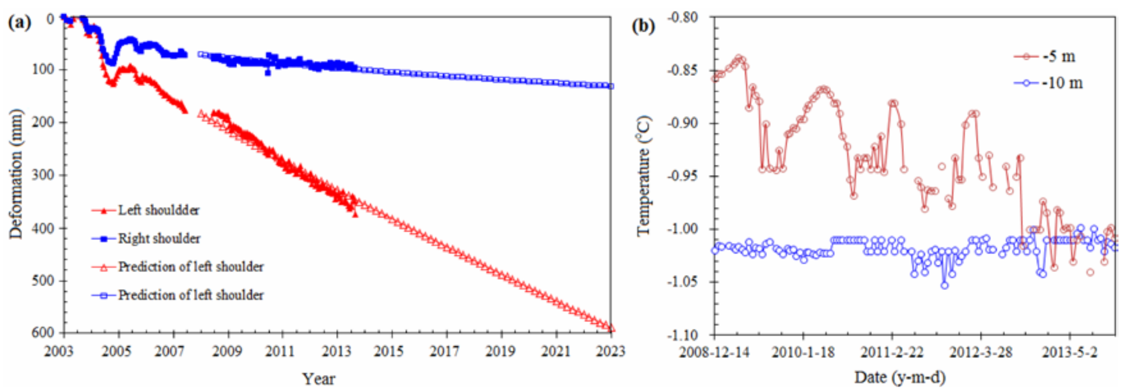

Figure 5. Deformation and ground temperature at section DK1041+258. (a) the field measured and predicted embankment settlement; (b) ground temperature changes at depths of 5 and 10 m on right shoulder.

Ground temperature changes at the depths of 5 and 10m at section DK1041+258 were shown in Figure 5b. Permafrost at depth of 5m on the right shoulder experienced obvious cooling from 2003 to 2014, with decreases of about 0.17 °C. However, ground temperature at depth of 10 m still unchanged in the past 11 years. It can be concluded that cooling of the CRBE was relatively limited and did not produce cooling effects strong enough to influence the deep permafrost.

3.3 Crushed-rock Sloped Embankment (CRSE)

In order to analyze the process of embankment settlements on CRSE, monitoring section DK1045+369 was chosen as an example. Figure 4a shows that both left and right shoulder had experienced significant settlement from 2003 to 2014. Among the 11 years monitoring period, the settlement on right and left embankment shoulder was 66 and 101 mm, and such settlement were mainly occurred before 2006. From 2003 to 2006, the settlement on right and left shoulder was 45 and 68 mm. To further analyze the long-term variations of embankment settlements, we predict the possible develop trend of embankment settlements as the method illustrated above. The predicted results indicate that the total embankment settlements on right and left embankment shoulders will reach 93 and 146 mm by the year 2023.

For the ground temperature, permafrost at the 5 and 10 m depths on the right shoulders experienced cooling of different magnitudes, with decreases of about 0.52 °C and 0.21 °C, respectively. It can be concluded that cooling of the CRSE was decreased with increasing of depth

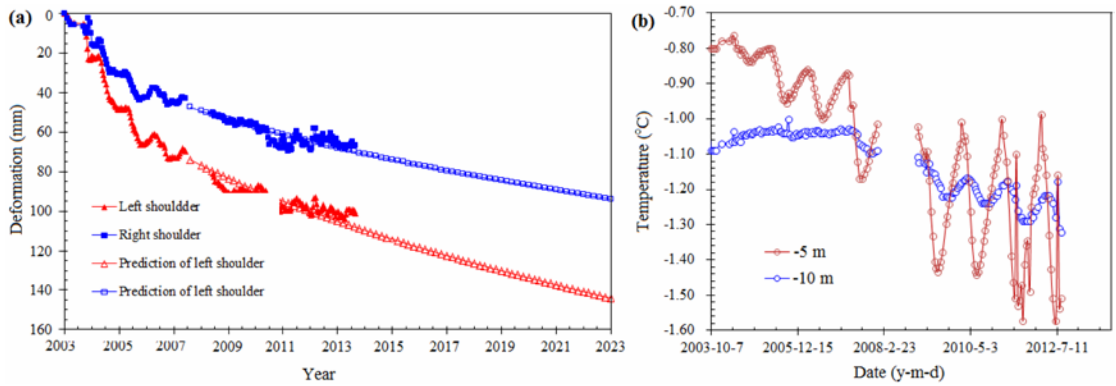

Figure 6. Deformation and ground temperature at section DK1045+369. (a) the field measured and predicted embankment settlement; (b) ground temperature changes at depths of 5 and 10 m on right shoulder.

3.4 U-shaped Crushed-rock Embankment (UCRE)

Figure 7a shows the process of embankment settlements of a typical UCRB at section DK1046+258. Both the left and right embankment shoulders had experienced significant settlement from 2003 to 2014. During the 11 years monitoring period, the settlement on right and left embankment shoulders were 55 and 115 mm, respectively, with MASR of the embankment were about 5.0 and 10.5 mm/a. The settlement on left embankment shoulder in the past 11 years could be divided into three stages: (1) a significant settlement occurred in the initial 2 years; (2) a nearly stable stage in the next 4 years; (3) obvious deformation in the last 5 years. However, the settlement on the right shoulder showed as sustained and slow increases from 2003 to 2006. The predicted embankment settlements in both two shoulders were also showed in Figure 7a. As the fitting results for the left shoulder are not satisfactory, so the predicted embankment settlements on the left shoulder may not accurate. However, the settlements in both two embankment shoulders will continuously increase in the future.

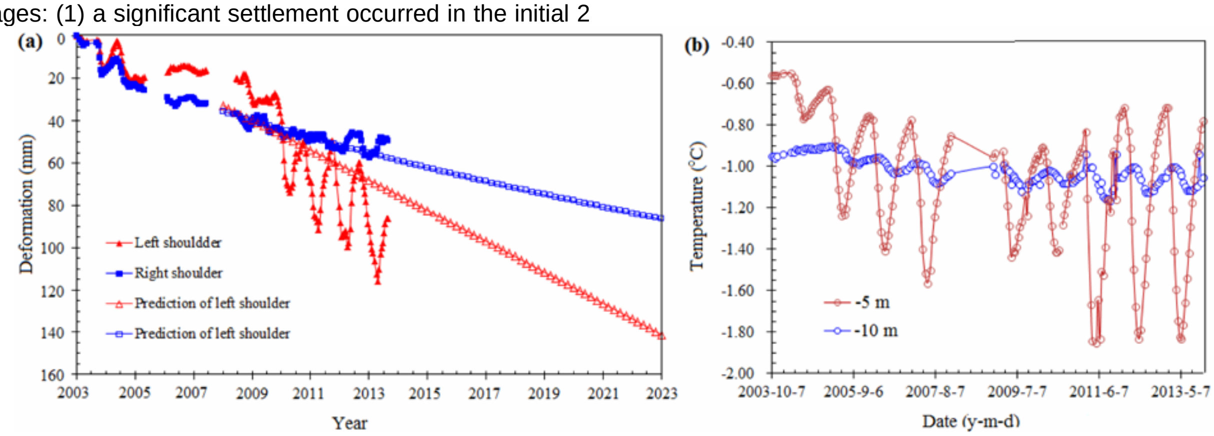

Figure 7. Deformation and ground temperature at section DK1046+258. (a) the field measured and predicted embankment settlement; (b) ground temperature changes at depths of 5 and 10 m on right shoulder

For the ground temperature in UCRE, the permafrost at depths of 5 and 10m show as a weak cooling process from 2003-2014 (Figure 7b), but the cooling effects at depth of 5m is more significant than the effects at depth of 10m. The cooling process of the UCRE at depth of 10m mainly includes two stages: (1) a weak warming of the underlying permafrost occurred in the initial 2 years, and (2) a weak but persistent cooling effect at the last 9 years.

4 DISCUSSION

Based on the above investigation and analyses, the embankment settlements and ground temperature changes for the four main types of embankment structures are summarized in Table 1. For TE, due to the low ice content of permafrost under the embankment, the magnitudes of embankment deformation was not much significant, but the underlying permafrost had some warming trends. The temperature increase of the frozen soils could lead to strength loss and increase in creep strains and creep strain rate (Anderland and Ladanyi, 2004). In addition, the monitoring and simulative results in Beiluhe Basin indicated that the embankment settlement could approach 300 mm after 50 years of construction (Zhang et al., 2007). So the settlement on TE will be considerable and hence should gain more attentions (Ma et al. 2011). For CRBE, it has a weak cooling effects on shallow permafrost, but the magnitudes of embankment settlements are much significant. The total settlements on the left shoulder had reached to 380 mm from 2003 to 2014, such big settlements will impact the long-term stability of embankment. For CRSE and UCRE, some settlements occurred on the embankment, but the magnitudes of them were not significant. Such settlements may be originated from underlying permafrost, which mainly attributed to creep of warm and ice-rich layer beneath permafrost table (Ma et al. 2011). However, this type of embankment structures had a obvious cooling effect on either shallow permafrost or deep permafrost, which will result in a continuous cooling process and the temperature of the underlying permafrost decreased steadily. As a result, the warm and ice-rich permafrost under the embankment will become cold and more stable, and thereby reduce the embankment settlements. Therefore, CRSE and UCRE are the best embankment of all the four monitored embankments. When take into account the symmetry of the embankment temperature distribution and long-term embankment stability, UCRE might be much better than CRSE.

In addition, the differential deformations of embankment between right and left shoulder were significant in the four types of embankment, especially in CRBE, the magnitudes of differential settlement had already exceeded 290 mm (Table 1). These differential deformations are mainly related to different temperature field under embankment (Ma et al., 2009). Two reasons might lead to different temperature field under the two embankment shoulders. First, different magnitudes of solar radiation absorbed by the two embankment slopes directly lead to thermal difference on the two slopes, and then result in temperature difference under the two shoulders. The left shoulder is the sunny slope and the right shoulder is the shady slope, so the solar radiation absorbed by left shoulder is more than right shoulder. Second, more than 70% of strong winds with a dominant northwest direction occur in winter on the QTP (Zhang et al., 2008), and the alignments of the monitored embankments are all approximately northeast to southwest. Therefore, the right shoulder and left shoulder would be windward and leeward slopes, respectively. As a result, wind-forced convection on the windward slope could produce considerable cooling effects during winter time.

Table 1. Comparison of embankment settlements and ground temperature changes among the four type of embankment structures

Embankment structure	Deformation (mm)		Ground temperature changes (^oC)	
	Left shoulder	Right shoulder	-5 m	-10 m
TE	95	55	-[1]	+0.19
CRBE	380	90	-0.17	-[1]
CRSE	68	45	-0.52	-0.21
UCRE	115	55	-0.60	-0.11

[1] unchanged

5 CONCLUSIONS

Based on the above analyses, the main conclusions are:

(1) Eleven years of monitored data show that the deformation of all the embankments generally shows as settlement. Among the four types of the embankments, the CRBE has the maximum settlement value, while the magnitudes of settlements for CRSE and UCRE were obviously less than CRBE. In addition, due to the low ice content of permafrost under the embankment, the magnitudes of embankment deformation for TE was also not much significant. For an embankment, different deformations occur between right and left shoulder, and these differential deformations mainly related to different temperature field under embankment.

(2) The predicted results of embankment settlement show that the long-term development of embankment deformation for CRBE is more significant than CRSE and UCRE, especially on the left shoulder.

(3) The underlying permafrost in TE had some warming trends from 2003 to 2014, and the CRBE only have weak cooling effects on shallow permafrost. However, CRSE and UCRE had obvious cooling effect on either shallow permafrost or deep permafrost.

(4) Considering the mechanical stability, cooling effect, symmetry of the ground temperature regime, material property and construction technique, UCRE is recommend for future application in roadbed construction in permafrost regions.

ACKNOWLEDGEMENTS

We gratefully acknowledge editors and two reviewers for their valuable and constructive comments and suggestions. This work was supported by the State Key Development Program of Basic Research of China (973 Plan, 2012CB026101), the Western Project Program of the Chinese Academy of Sciences (KZCX2-XB3-19), the Foundation for Innovative Research Groups of the National Natural Science Foundation of China (Grant No. 41121061), and the National Sci-Tech Support Plan (2014BAG05B05).

REFERENCES

Anderland, Orlando B., Ladanyi, Branko, 2004. Frozen Ground Engineering. John Wiley & Sons. Inc., Hoboken, New Jersy.

Cheng G D. 2003. Construction of Qinghai-Tibet Railway with cooled roadbed. China Railway Science (in Chinese), 24: 1–4

Chen G D. 2005. A roadbed cooling approach for the construction of Qinghai-Tibet Railway. Cold Regions Science and Technology, 42: 169–176

Cheng G D, Sun Z Z, Niu, F J. 2008. Application of the roadbed cooling approach in Qinghai-Tibet railway engineering. Cold Regions Science and Technology, 53: 241–258

Feng W J, Ma W, Li D Q, et al. 2006. Application investigation of awning to roadway engineering on the Qinghai-Tibet Plateau. Cold Regions Science and Technology, 45: 51–58

Ma W, Cheng G D, Wu Q B. 2002. Preliminary study on technology of cooling foundation in permafrost regions (in Chinese). Journal of Glaciology and Geocryology, 24: 579–587

Ma, W., Cheng, G.D., Wu, Q.B., 2009. Construction on permafrost foundations: lessons learned from the Qinghai–Tibet Railroad. Cold Regions Science and Technology 59 (1), 3–11.

Ma, W., Mu, Y., Wu, Q., Sun, Z., & Liu, Y. (2011). Characteristics and mechanisms of embankment deformation along the Qinghai–Tibet Railway in permafrost regions. Cold Regions Science and Technology, 67(3), 178-186.

Ma W, Mu Y H, Li G Y, et al. 2013. Responses of embankment thermal regime to engineering activities and climate change along the Qinghai-Tibet Railway (in Chinese). Sci China Earth Sci, 43: 478–489

Mu Y H, Ma W, Wu Q B, et al. 2012. Cooling processes and effects of crushed rock embankment along the Qinghai-Tibet Railway in permafrost regions. Cold Regions Science and Technology, 78: 107–114

Niu F J, Cheng G D, Yu Q H. 2004. Ground-temperature controlling effects of duct-ventilated railway embankment in permafrost regions(in Chinese). Sci China Ser D-Earth Sci, 47(Suppl): 152–160

Niu F J, Cheng G D, Xia H M, et al. 2006. Field experiment study on effects of duct-ventilated railway embankment on protecting the underlying permafrost. Cold Regions Science and Technology, 45: 178–192

Wu Q B, Cheng G D, Ma W. 2004. Impact of permafrost change on the Qinghai-Tibet Railraod engineering, Sci China Ser D-Earth Sci, 47(Suppl): 122–130

Zhang T J, Baker T H W, Cheng G D, et al. 2008. The Qinghai–Tibet Railroad: a milestone project and its environmental impact. Cold Regions Science and Technology, 53: 229–240

Zhang, J.M., Liu, D., QI, J.L., 2007. Estimation on the settlement and deformation of embankment along Qinghai–Tibet Railway in permafrost regions. China Railway Science 28 (3), 12–17 (in Chinese with English abstract).